

pubs.acs.org/JPCA Article

Microwave Study of Triflic Acid Hydrates: Evidence for the Transition from Hydrogen-Bonded Clusters to a Microsolvated Ion Pair

Anna K. Huff, Nathan Love, and Kenneth R. Leopold*



Cite This: J. Phys. Chem. A 2021, 125, 8033-8046



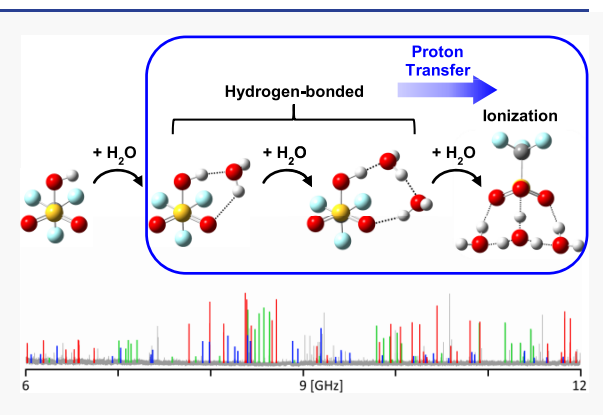
ACCESS

III Metrics & More

Article Recommendations

s Supporting Information

ABSTRACT: Rotational spectra of the mono-, di-, and trihydrates of triflic acid, $CF_3SO_3H\cdots(H_2O)_{n=1-3}$, have been recorded by pulsed nozzle Fourier transform microwave spectroscopy and spectroscopic constants obtained have been compared with values calculated at several levels of theory. The experimental results are consistent with the theoretical predictions presented here and elsewhere, indicating that with only one or two water molecules, triflic acid remains un-ionized in a cold molecular complex. The experiments further concur with theoretical predictions that the addition of a third water molecule transforms the system into what is best regarded as a hydrated hydronium triflate ion pair. Thus, only three water molecules are needed to induce ionization of triflic acid in a cold molecular cluster. This number is somewhat low compared with that for other simple protic acids and likely reflects the superacidity of triflic acid. Simple energetic arguments can be used to rationalize this result.



INTRODUCTION

The sequential hydration of protic acids in the gas phase is an interesting venue in which to explore the relationship between aggregation and reactivity. For most simple mineral acids which ionize in aqueous solution, complexation with a small number of water molecules is insufficient to induce the proton transfer seen in the bulk phase. Indeed, for many simple protic acids that readily ionize in liquid water, the number of water molecules needed before evidence of proton transfer can be found in an $HA\cdots(H_2O)_n$ cluster is typically in the 3–5 range. A logical interpretation of this observation is that some number of (micro)solvent molecules is needed to stabilize the charge separation associated with the proton transfer.

A large number of computational studies have been performed to explore the effects of sequential hydration of simple acids such as HNO_3 , H_2SO_4 , HF, HCl, HBr, and HI. References to work prior to 2011 may be found in an earlier review. Several examples of the numerous subsequent works on these and other acids can be found in refs 2–13 and references therein. Of particular relevance to the present study is a series of calculations involving the hydration of triflic acid, CF_3SO_3H . Triflic acid differs from many of the more common acids studied in that it is an extraordinarily strong proton donor, i.e., a "superacid." Indeed, based on Hammett acidity functions, triflic acid is 2–3 orders of magnitude stronger than sulfuric acid. The theoretical studies find that for the complexes $CF_3SO_3H\cdots(H_2O)_n$ with n=1 and 2, the lowest energy forms in the gas phase consist of hydrogen-

bonded rings, a motif that is common for the hydrates of unionized acids. However, at n=3, the proton-transferred structure, $CF_3SO_3^-\cdots H_3O^+(H_2O)_2$, becomes the lowest energy form. The same theoretical result is also obtained for halosulfonic acids $(XSO_3H, X = F, Cl, Br)$. This is somewhat unusual insofar as many common acids require a larger number of water molecules, though a notable exception lies in several hydrated sulfur oxoacids, for which calculations indicate that ionized forms represent local or global minimum energy structures at n=2. Still, the number of water molecules needed to ionize triflic acid is predicted to be what one might term "on the low end of typical."

It is interesting to note that there are also crystallographic studies of several triflic acid hydrates, including the monohydrate, dihydrate, tetrahydrate, and hemihydrate. Curiously, it appears that there are no reports of analogous studies of the trihydrate. For all of these systems, in which the local environment is fully developed relative to that in a gas-phase cluster, the triflic acid is ionized, and the crystal thus contains $CF_3SO_3^-$ anions. These triflic acid hydrates have been used to explore the nature of hydrated protons in the

Received: August 1, 2021 Revised: August 20, 2021 Published: September 3, 2021



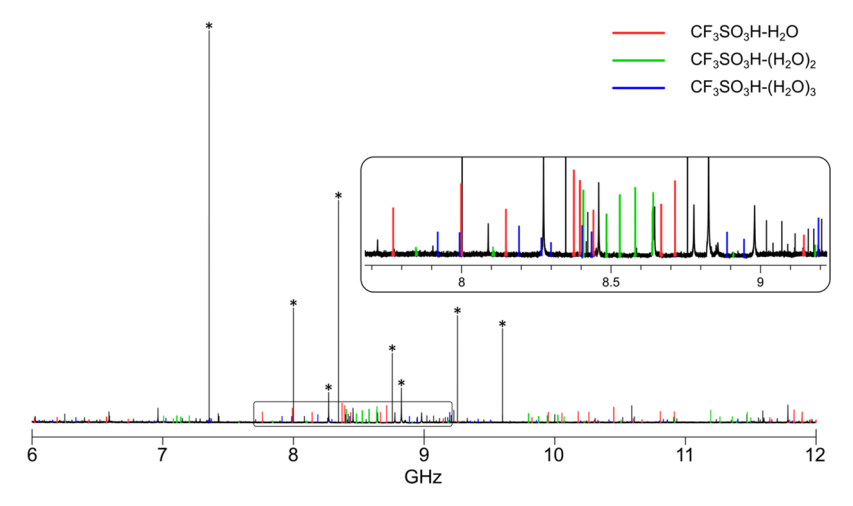


Figure 1. 6–12 GHz portion of the chirped-pulse spectrum of CF_3SO_3H and H_2O in argon. This spectrum represents the average of 180 000 free-induction decay (FID) signals, each collected for 20 μ s. The inset shows a zoomed-in portion of the broadband spectrum from about 7.7 to 9.2 GHz. Lines assigned to the triflic acid monohydrate, dihydrate, and trihydrate are highlighted in red, green, and blue, respectively. Strong lines designated with an asterisk are a combination of $(H_2O)_2$ and $Ar\cdots(H_2O)_2$ transitions as well as instrumental artifacts. The remaining lines arise from triflic acid monomer, weaker transitions of $(H_2O)_2$ and $Ar+H_2O$ species, and additional instrument artifacts.

solid state, ^{25–27} and the protonation of sulfonate groups finds applications in the design and development of fuel cells. ²⁸

In this paper, we report the gas-phase observation of the microwave spectra of the mono-, di-, and trihydrates of triflic acid, $CF_3SO_3H\cdots(H_2O)_n$ (n=1-3). Moreover, while the computational studies noted above have been quite thorough, further calculations are reported which are particularly tailored to facilitating the direct comparison between the theory and the experimental spectra of this work. The computational results concur with earlier studies, and the experimental results provide direct support for the predicted transition from hydrogen bonding to ion pair formation when the hydration number increases from 2 to 3. We conclude with a simple model that provides an intuitive understanding of the hydration number necessary to induce ionization.

■ EXPERIMENTAL METHODS AND RESULTS

Rotational spectra of the triflic acid hydrates were collected using a combined cavity²⁹ and chirped-pulse³⁰ Fourier transform microwave spectrometer, details of which have been given elsewhere.^{31,32} Transition frequencies obtained on the chirped-pulse system were typically accurate to ~12 kHz, while those obtained in the cavity mode of the spectrometer were accurate to ~3 kHz. In the case of di-deuterated isotopologues, however, the dense deuterium hyperfine structure decreased the measurement accuracy such that only approximate line centers could be obtained. In these cases, the measurement uncertainties varied between 3 and 6 kHz, depending on the transition.

To produce complexes, water vapor was entrained in argon gas by passing the latter through liquid water and expanding the resulting mixture through a stainless steel 0.8 mm diameter orifice cone nozzle at a stagnation pressure of 1.2 atm. Triflic acid vapor was separately introduced by continuously flowing argon at a pressure of 0.4 atm over a few milliliters of liquid triflic acid (98%, TCI Chemical) and injecting the vapor along the axis of the expansion a few millimeters downstream from the 0.8 mm orifice through a 0.016 in. inner diameter hypodermic needle, as described in previous work.³³ Because of the corrosive nature and relatively low vapor pressure of

triflic acid (~8 Torr at 25 °C), the liquid triflic acid was contained in a small stainless steel reservoir located only a few inches upstream of the injection end of the hypodermic needle. ³⁴S spectra, when observed, were obtained in natural abundance. The deuterated complexes, CF₃SO₃H····D₂O, CF₃SO₃D···DOH, and CF₃SO₃H···(D₂O)₂, were observed using the same conditions above except that argon was passed through liquid D₂O (Cambridge Isotope Laboratories, 99.9%). For CF₃SO₃H···DOH, a 1:1 molar ratio of H₂O and D₂O was prepared. The CF₃SO₃D···DOH species was unexpectedly observed from the apparent H/D exchange of normal triflic acid and D₂O in the supersonic jet. Interestingly, such H/D exchange was not observed in analogous experiments on the HNO₃···H₂O complex. ³⁴ A portion of the chirped-pulse spectrum of the parent species between 6 and 12 GHz is shown in Figure 1.

Triflic Acid Monohydrate. Spectra of the triflic acid monohydrate were identified by the triflic acid and water dependence of the signals, the agreement between observed and predicted rotational constants, and the agreement between the observed and predicted changes in the rotational constants upon isotopic substitution. These comparisons will be discussed more thoroughly in the next section. Two states were observed for both the parent and 34S isotopologues. These states appeared as spectral pairs separated by about 100-300 kHz, with the separation generally increasing at higher J. A trace of the $5_{15} \leftarrow 4_{04}$ transition for $CF_3SO_3H\cdots$ H₂O illustrating the splitting is shown in Figure 2. This type of splitting is common for water complexes undergoing internal motion that exchanges the roles of the bound and free hydrogens. In the present case, the lower frequency line was always more intense than the higher frequency line (though for some weaker transitions, the latter could not be observed at all). Although spectral intensities in cavity measurements are highly sensitive to the offset relative to the tuned cavity frequency, relative intensities were generally observed to be in the approximately 3:1 ratio expected from proton nuclear spin statistics. On this basis, the lower and higher frequency transitions were assigned to the 0⁻ and 0⁺ states, respectively. The two states were fit separately using a semirigid rotor

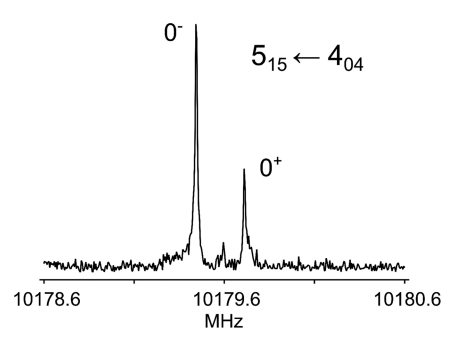


Figure 2. Cavity spectrum of the $5_{15} \leftarrow 4_{04}$ transition for $CF_3SO_3H\cdots H_2O$ resulting from the average of 2000 free-induction decay signals, which were each collected for 140.8 μs . The 0^+ and 0^- labels refer to the symmetric and antisymmetric tunneling states arising from internal water motion. The small feature between the pair of lines is an artifact from the cavity frequency.

Watson A-reduced Hamiltonian³⁵ in the I^r representation using the SPFIT program of Pickett.³⁶ For the parent species, lines were measured from both cavity and chirped-pulse spectra with frequencies ranging 4–18 GHz. Both a- and b-type transitions were observed with J''=1-8 and $K_a''=0-4$. No c-type transitions were observed.

The majority of transitions for the remaining isotopologues were measured exclusively on the cavity spectrometer to take advantage of the higher sensitivity and resolution. For these isotopologues, both a- and b-type spectra were observed and included rotational transitions up to J'' = 6 and up to $K_a'' = 3$. The spectra of CF₃SO₃H···D₂O were too congested to assign deuterium hyperfine structure or identify tunneling states, so only the approximate line centers were obtained. Deuterium hyperfine structure was, however, resolved for CF₃SO₃H···· DOH and nuclear quadrupole coupling constants were determined. Once the hyperfine structure was assigned, no additional lines remained that could be attributed to a second state. For CF₃SO₃D···DOH, small splittings (less than 40 kHz) were observed that matched the predicted hyperfine structure from the two deuterium atoms. However, an insufficient number of components were resolved to fit the nuclear

quadrupole coupling constants. As with CF₃SO₃H···DOH, there did not appear to be lines remaining after accounting for the small splittings with the predicted deuterium hyperfine structure. This disappearance of the second state with single deuterium substitution on the water moiety confirms that the splitting observed for the parent and ³⁴S complexes arises from a water tunneling motion that interchanges the bound and free hydrogens. Frequencies, assignments, and residuals from the least-squares fits are provided in the Supporting Information. The resulting spectroscopic constants for all isotopologues studied are given in Table 1.

Triflic Acid Dihydrate. The $CF_3SO_3H\cdots(H_2O)$, spectrum was initially observed as a prominent a-type spectrum in the broadband chirped-pulse spectrum. As with the monohydrate, it was identified by its dependence on the presence of triflic acid and water, as well as by the comparison between observed and calculated rotational constants and isotope shifts. Weaker b-type transitions were also located in the broadband spectrum after obtaining a preliminary fit of the stronger a-type lines. Once a more robust fit was achieved, additional weaker transitions, including both b-type lines and a-type transitions involving higher K_{av} were readily located with the cavity spectrometer. In total, 50 transitions were observed for $CF_3SO_3H\cdots(H_2O)_2$ between 4 and 16 GHz and included J" = 2-10 and K_a'' = 0-3. No evidence of internal motion was observed, and careful searches for c-type spectra were unsuccessful, indicating a small (or vanishing) value of μ_c . Once spectra of the parent species were fit, transitions from the ³⁴S isotopologue were located and measured in natural abundance using the cavity spectrometer. These, again, included both a- and b-type lines and accessed J'' = 4-7 and $K_a'' = 0-2$. For $CF_3SO_3H\cdots(D_2O)_2$, lower signal-to-noise ratios restricted the observed spectra to only a-type transitions involving J'' = 4-8 and $K_a'' = 0-2$. Observed frequencies, assignments, and residuals are given in the Supporting Information. Spectroscopic constants for the parent and isotopically substituted species studied are given in Table 2.

Triflic Acid Trihydrate. After the triflic acid mono- and dihydrate spectra were assigned and accounted for in the chirped-pulse spectrum, another *a*-type spectrum remained

Table 1. Spectroscopic Constants of Observed CF₃SO₃H···H₂O Isotopologues^a

	CF ₃ SO ₃	$H \cdot \cdot \cdot H_2O$	CF ₃ ³⁴ SO	₃ H···H ₂ O			
	0 ⁻ state	0 ⁺ state	0 ⁻ state	0+ state	$CF_3SO_3H\cdots D_2O$	CF ₃ SO ₃ H···DOH	CF ₃ SO ₃ D···DOH
A (MHz)	1853.10915(22)	1853.16271(39)	1844.65876(38)	1844.70981(86)	1819.5276(27)	1845.5867(32)	1837.0311(15)
B (MHz)	1144.85988(10)	1144.87119(14)	1144.56767(16)	1144.57991(88)	1102.56191(36)	1123.83590(73)	1114.44376(52)
C (MHz)	959.540437(79)	959.56454(10)	957.08772(13)	957.11185(42)	923.43851(33)	945.28415(36)	939.13617(25)
Δ_{J} (kHz)	0.6302(14)	0.6295(18)	0.6247(18)	0.651(19)	0.6540(45)	0.5867(88)	0.6003(41)
Δ_{JK} (kHz)	-2.3875(74)	-2.379(11)	-2.417(18)	-2.560(94)	-2.558(98)	-2.21(11)	-2.197(22)
Δ_K (kHz)	3.639(39)	3.606(67)	[3.639]	[3.606]	[3.627]	3.48(27)	3.70(10)
δ_{J} (kHz)	0.21389(70)	0.21195(97)	0.2165(16)	0.228(12)	0.2216(30)	0.1994(68)	0.1919(24)
δ_K (kHz)	0.307(19)	0.297(25)	[0.307]	[0.297]	[0.295]	[0.295]	0.403(49)
χ_{aa} (MHz)						-0.142(20)	
$(\chi_{bb} - \chi_{cc})$ (MHz)						-0.508(35)	
N^b	84	64	20	14	18	24 (47)	28
RMS $(kHz)^c$	5.4	3.4	0.9	2.0	2.0	4.0	3.6

"Numbers in brackets are fixed to the value determined in the parent fit. Since tunneling states were not observed for the $CF_3SO_3H\cdots D_2O$ and $CF_3SO_3H\cdots DOH$ species, the values of Δ_K and δ_K were derived from a separate fit of the parent species using the average of the 0^+ and 0^- frequencies to simulate a parent value, had the states not been resolved. (Any rotational transitions for which the weaker state was not observed were omitted.) bNumber of transitions included in fit. For $CF_3SO_3H\cdots DOH$, the number in parentheses indicates the number of hyperfine components. This is the only isotopologue with resolved hyperfine structure. Root-mean-square (RMS) deviation of the value of the observed minus calculated frequencies from the least-squares fit.

Table 2. Spectroscopic Constants of Observed CF₃SO₃H···(H₂O), Isotopologues^a

	$CF_3SO_3H\cdots(H_2O)_2$	$CF_3^{34}SO_3H\cdots(H_2O)_2$	$CF_3SO_3H\cdots(D_2O)_2$
A (MHz)	1467.5486(28)	1461.1896(61)	1426.303(52)
B (MHz)	730.94197(26)	730.85224(95)	689.0174(12)
C (MHz)	691.42664(21)	689.92802(39)	655.62423(74)
$\Delta_I ext{ (kHz)}$	0.40870(64)	0.4092(36)	0.3733(58)
Δ_{JK} (kHz)	-0.611(13)	-0.507(39)	-0.63(12)
Δ_K (kHz)	2.89(72)	[2.89]	[2.89]
$\delta_{J}~(\mathrm{kHz})$	0.04586(58)	0.0517(43)	0.0206(57)
$\delta_{K} ext{ (kHz)}$	-1.389(46)	[-1.389]	[-1.389]
N^b	50	14	16
RMS $(kHz)^c$	4.1	1.6	4.0

[&]quot;Numbers in brackets are fixed to the value determined in the parent fit. ^bNumber of transitions included in fit. ^cRoot-mean-square deviation of the value of the observed minus calculated frequencies from the least-squares fit.

and was found to be readily attributable to the triflic acid trihydrate. The 37 *a*-type transitions were measured between 6 and 12 GHz and include J''=5-11 and $K_a''=0-3$. Spectroscopic constants are presented in Table 3. The signals

Table 3. Spectroscopic Constants of CF₃SO₃H···(H₂O)₃

	$CF_3SO_3H\cdots(H_2O)_3$
A (MHz)	1353.4599(50)
B (MHz)	546.99304(30)
C (MHz)	482.05570(23)
$\Delta_{J}~(\mathrm{kHz})$	0.0214(10)
$\delta_{J} ext{ (kHz)}$	0.00488(67)
N^a	37
RMS $(kHz)^b$	5.4

^aNumber of transitions included in fit. ^bRoot-mean-square deviation of the value of the observed minus calculated frequencies from the least-squares fit.

were weaker than those of the dihydrate, as expected, and did not always appear in the chirped-pulse spectrum. However, they were consistently observable with the higher sensitivity of the cavity system. Indeed, additional scans on the cavity spectrometer enabled the observation of two weak c-type transitions at the frequencies predicted by the fit to the a-type spectra alone. Careful scans in the vicinity of several b-type transitions, however, did not produce any spectra, indicating a small (or vanishing) value of μ_b . No spectra were observed for isotopically substituted species. Frequencies, assignments, and residuals are provided in the Supporting Information.

COMPUTATIONAL METHODS AND RESULTS

As noted in the Introduction section, gas-phase $CF_3SO_3H\cdots(H_2O)_n$ (n=1-6) clusters have been previously investigated by computational methods, $^{14-16}$ but calculations for $CF_3SO_3H\cdots(H_2O)_n$ (n=1-3) were repeated at various levels of theory to obtain predictions specifically relevant to rotational spectroscopy. All calculations were performed using Gaussian $16.^{37}$ More than one low-lying structure exists for each triflic acid hydrate presented here, and the results for each species are discussed below. The structural predictions agree with those of previous studies, $^{14-16}$ and DSD-PBEP86-D3BJ/jun-cc-pVTZ optimized structures are given in Figures 3-5 as a convenience to facilitate the discussion. Additional density functional theory (DFT) methods were used to obtain the minimum energy structures, rotational constants, and dipole moments so that comparisons with the experiment

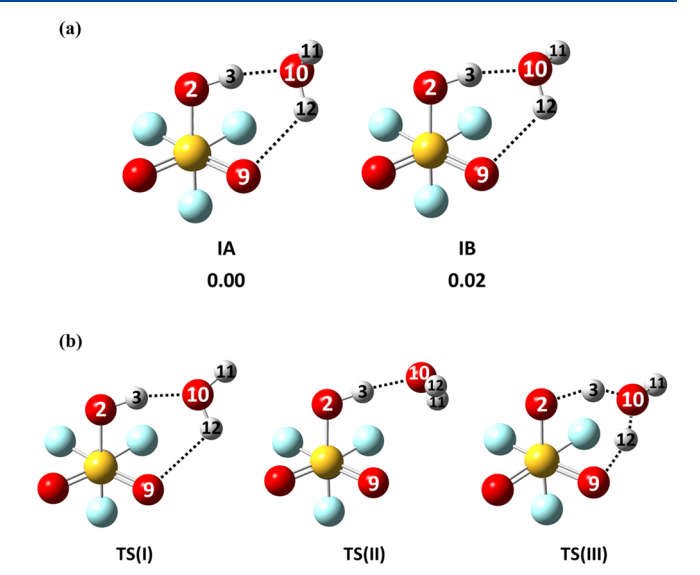


Figure 3. (a) Two lowest energy conformers of CF₃SO₃H····H₂O calculated at the DSD-PBEP86-D3BJ/jun-cc-pVTZ level of theory. Numbers give the relative energies in kcal/mol after zero-point corrections. Here, IA is lower in energy than IB by only 0.02 kcal/mol after zero-point energy corrections and the two conformers are therefore effectively isoenergetic. A complete tabulation of conformer energies at all levels of theory used is given in Table 4. (b) Three transition-state structures of CF₃SO₃H····H₂O calculated at the DSD-PBEP86-D3BJ/jun-cc-pVTZ level of theory. TS(I) is 0.27 kcal/mol lower in energy than the minimum energy conformer (after ZPE corrections), while TS(II) and TS(III) lie 0.53 and 11.0 kcal/mol higher in energy, respectively. A complete tabulation of transition-state energies at all levels of theory used is given in Table 5.

would not rely on a single level of theory. The methods were chosen based on excellent performance demonstrated in recent rotational spectroscopic work³⁸ and include the B2PLYP-D3BJ/jun-cc-pVTZ and the B3LYP-D3BJ/def2-TZVP computational models.^{39–43} M06-2X/6-311++G(3df,3pd) calculations were also performed. Additionally, anharmonic frequency and vibration-rotation calculations at the B3LYP-D3BJ/jun-cc-pVDZ level were performed to apply vibrational contributions to the rotational constants at all levels of the theory presented. For methods with the jun-cc-pVnZ (n = D, T) basis set, the jun-cc-pV(n+d)Z basis set was obtained from the Basis Set Exchange library⁴⁴ and used on sulfur atoms to include an additional set of tight d functions (jun-cc-pVnZ is applied to all other atoms). The energies of the predicted conformers relative to the free monomers at the various levels of theory,

Table 4. Relative Energies of Conformers of $CF_3SO_3H\cdots(H_2O)_{n=1-3}$ at Various Levels of Theory Uncorrected and Corrected for Zero-Point Energy $(ZPE)^{ab}$

		06-2X ·G(3df,3pd)		P-D3BJ -TZVP		TP-D3BJ c-pVDZ ^b		YP-D3BJ c-pVTZ ^b		EP86-D3BJ c-pVTZ ^b
	ΔE	ΔE + ZPE	ΔE	ΔE + ZPE	ΔE	ΔE + ZPE	ΔE	ΔE + ZPE	ΔE	ΔE + ZPE
rel. to $CF_3SO_3H + H_2O$										
CF ₃ SO ₃ H····H ₂ O IA	-14.95	-12.82	-15.27	-13.03	-14.72	-12.57	-12.46	-10.31	-12.37	-10.22
CF ₃ SO ₃ H···H ₂ O IB	-15.05	-12.87	-15.36	-13.11	-14.77	-12.62	-12.46	-10.31	-12.36	-10.20
rel. to $CF_3SO_3H + 2H_2O$										
$CF_3SO_3H\cdots(H_2O)_2$ IIA	-33.40	-29.42	-30.29	-25.88	-29.22	-24.93	-23.87	-19.58	-23.36	-19.07
$CF_3SO_3H\cdots(H_2O)_2$ IIB	-33.36	-29.39	-30.17	-25.77	-29.08	-24.80	-23.73	-19.46	-23.18	-18.91
$CF_3SO_3H\cdots(H_2O)_2$ IIC	-32.78	-28.81	-29.57	-25.29	-28.56	-24.43	-23.34	-19.21	-22.83	-18.71
$CF_3SO_3H\cdots(H_2O)_2$ IID	-32.65	-28.70	-29.42	-25.15	-28.45	-24.28	-23.35	-19.19	-22.84	-18.68
rel. to $CF_3SO_3H + 3H_2O$										
$CF_3SO_3H\cdots(H_2O)_3$ IIIA	-50.53	-43.57	-46.69	-39.16	-45.32	-37.97	-34.73	-27.38	-33.69	-26.34
$CF_3SO_3H\cdots(H_2O)_3$ IIIB	-50.36	-43.45	-46.58	-39.02	-45.23	-37.83	-34.61	-27.21	-33.58	-26.18
$CF_3SO_3H\cdots(H_2O)_3$ IIIC	-46.35	-40.66	-42.15	-35.83	-40.90	-34.70	-32.49	-26.28	-31.58	-25.38
$CF_3SO_3H\cdots(H_2O)_3$ IIID	-46.84	-40.94	-42.25	-35.78	-40.95	-34.36	-30.14	-23.55	-29.16	-22.57

[&]quot;Energies are in kcal/mol and are relative to the sum of the respective monomers. Energies without zero-point correction are designated by ΔE , and energies with ZPE corrections are designated by $\Delta E + ZPE$. For B2PLYP-D3BJ and DSD-PBEP86-D3BJ calculations with the jun-cc-pVTZ basis set, $\Delta E + ZPE$ were obtained using zero-point energies from B3LYP-D3BJ/jun-cc-pVDZ frequency calculations. For calculations using jun-cc-pVDZ or jun-cc-pVTZ basis sets, jun-cc-pV(D+d)Z or jun-cc-pV(T+d)Z basis sets, respectively, were used on the sulfur atom.

Table 5. Energy Barriers for CF₃SO₃H····H₂O Transition-State Structures at Various Levels of Theory abc

		energy relative to global minimum $(kcal/mol)^c$								
	M06-2X 6-311++G(3df,3pd)				CYP-D3BJ cc-pVDZ ^d			DSD-PBEP86-D3BJ jun- cc-pVT \mathbf{Z}^d		
	ΔE	ΔE + ZPE	ΔE	ΔE + ZPE	ΔE	ΔE + ZPE	ΔE	ΔE + ZPE	ΔE	ΔE + ZPE
CF ₃ SO ₃ H····H ₂ O TS(I)	0.82	0.27	0.81	0.30	0.57	0.09	0.29	-0.18	0.20	-0.27
$CF_3SO_3H\cdots H_2O\ TS(II)$	1.1	0.75	0.93	0.63	0.88	0.60	0.79	0.51	0.82	0.53
$CF_3SO_3H\cdots H_2O TS(III)$	8.4	6.9	8.5	7.0	8.2	6.8	11.9	10.5	12.4	11.0

^aFor B2PLYP-D3BJ and DSD-PBEP86-D3BJ calculations with the jun-cc-pVTZ basis set, the ZPE correction was obtained from B3LYP-D3BJ/jun-cc-pVDZ frequencies. ^bTransition-state structures are shown in Figure 3b. ^cFor each level of theory, the zero of energy is taken as the lowest minimum on the potential energy surface obtained at that level. ^dFor calculations using jun-cc-pVDZ or jun-cc-pVTZ basis sets, the jun-cc-pV(D + d)Z or jun-cc-pV(T+d)Z basis set was used on the sulfur atom, respectively.

both with and without zero-point energy (ZPE) corrections, are given in Table 4.

Triflic Acid Monohydrate. Two structures consistently converged to real minima for the triflic acid monohydrate. The structures are shown in Figure 3a and are labeled IA and IB. In both structures, there appears to be a primary hydrogen bond between the acidic proton of the triflic acid and the water oxygen, as well as a secondary hydrogen bond between a water hydrogen and the nearest oxygen on the sulfur. At all levels of theory, the primary hydrogen bond length is ~ 1.6 Å and the secondary hydrogen bond length is ~2.2 Å. In IA, the unbound hydrogen is oriented away from the CF3 group, while in structure IB, it is oriented toward the CF3 group. The difference in energies between these conformers is quite small, ranging only from ~0.0 to 0.1 kcal/mol among the levels of theory employed, with or without ZPE corrections. Out of the five sets of calculations, only DSD-PBEP86-D3BJ calculations predict IA to be more stable than IB, but only by 0.01 or 0.02 kcal/mol, depending on whether or not ZPE corrections were included. Practically speaking, these energy differences are small enough that the two structures are effectively isoenergetic. Note that this suggests the absence of any appreciable additional hydrogen bond between the unbound OH of water and a CF₃ fluorine. Indeed, the distance between the unbound water hydrogen and the nearest fluorine for IB is

quite long, ranging from 3.29 to 3.61 Å across the levels of theory tested.

Two transition states that connect structures IA and IB were also identified at all levels of the theory presented. The structures are shown in Figure 3b and the corresponding energies are included in Table 5. The first transition state, TS(I), involves a motion where the unbound water hydrogen wags back and forth between the orientations of structures IA and IB, as if the system switches the sp³ lone pair on water to which the triflic acid is hydrogen-bonded. (The hydrogen atom in the secondary hydrogen bond remains in the secondary hydrogen bond.) In contrast, the second transition state, TS(II), involves a motion that breaks the intermolecular interaction between the bound water hydrogen and one of the S=O oxygen atoms. The water molecule effectively rotates about the primary hydrogen bond and interconverts the bound and free water hydrogens. Without ZPE corrections, the barrier for TS(I) ranges from 0.20 to 0.82 kcal/mol. With ZPE corrections, however, the highest value for the barrier is 0.30 kcal/mol and goes down to lying 0.27 kcal/mol below the global minimum at some levels of theory. The calculated barriers are higher overall for TS(II) with a spread from 0.79 to 1.1 kcal/mol (0.51–0.75 kcal/mol with ZPE corrections).

Attempts to identify a proton-transferred minimum energy structure with all real frequencies were unsuccessful.

Table 6. Comparison between Observed Rotational Constants for Parent Triflic Acid Monohydrate and Theoretical Values for Predicted Conformers ab

			B2PLYP-D3BJ	DSD-PBEP86-D3BJ	RMS%
			jun-cc-pVTZ ^c	jun-cc-pVTZ c	
A (observed)		1853.10915(22)			
IA			1866	1866	0.9
			1864	1864	0.9
IB			1838	1837	1.5
			1829	1828	2.0
B (observed)		1144.85988(10)			
IA			1123	1139	2.2
			1104	1120	3.5
IB			1141	1159	2.3
			1127	1144	2.2
C (observed)		959.540437(79)			
IA			951	961	1.6
			938	948	2.4
IB			957	967	1.7
			945	956	1.8
$ \mu_a $		$\neq 0^e$			
$ \mu_b $		$\neq 0^e$			
$ \mu_c $		$\ll \mu_a, {\mu_b}^e$			
IA	(μ_a, μ_b, μ_c)		$(3.7, 1.9, 0.0^f)$	$(3.7, 2.0, 0.0^f)$	
IB	(μ_a, μ_b, μ_c)		(2.2, 3.8, 0.2)	(2.1, 3.8, 0.2)	

"Fitted rotational constants of the 0⁻ state and qualitative observations about dipole moment components are in bold. Table 1 shows the complete set of fitted spectroscopic constants for triflic acid monohydrate. Rotational constants are in MHz. Dipole moment components are in debye. Equilibrium rotational constants calculated for each level of theory are presented in the first row for A, B, and C. Vibrational ground-state rotational constants were calculated using the vibrational corrections at the B3LYP-D3BJ/jun-cc-pVDZ level/basis and are given in the second row for A, B, and C. For calculations using the jun-cc-pVDZ or jun-cc-pVTZ basis sets, the jun-cc-pV(D+d)Z or jun-cc-pV(T+d)Z basis set was used on the sulfur atom, respectively. ^dRMS percent deviation of calculated rotational constants relative to observed values among the five levels of theory used. The Supporting Information shows a full table of calculated constants. ^eFrom the observation of a- and b-type transitions. No c-type transitions were observed. ^fThe dipole moment component along the principal c-axis is not identically zero.

Optimization of a proton-transferred starting geometry terminated as a transition state with an imaginary frequency corresponding to proton transfer (TS(III) in Figure 3b). Equivalent transition states were identified for geometries in which the bound hydrogen is in the IA or IB orientation. Transition-state energies are given in Table 5. In both cases, the transition state lies 8.2-12.4 kcal/mol above the minimum (6.8-11.0 kcal/mol) with ZPE corrections). Note that there is no transition state that involves the acidic hydrogen simply shuttling between the OH oxygen of the triflic acid and water, which would lead to $\text{CF}_3\text{SO}_3^-\cdots\text{H}_3\text{O}^+$. Rather, the transition state is one in which the triflic acid hydrogen becomes a water hydrogen and water hydrogen becomes the triflic acid hydrogen on a different oxygen atom.

Finally, Table 6 compares the observed rotational constants with the theoretically predicted values for two of the five methods employed. Comparisons for all five methods are provided in the Supporting Information. The right-most column of Table 6 gives the RMS percent error in the equilibrium and vibrationally corrected computational values relative to the observed values among all five methods for each rotational constant (A, B, and C) and for each conformer (IA and IB). Also included are absolute values of the calculated components of the dipole moment along the inertial axes of the parent isotopologue $(\mu_{av}, \mu_{bv}, \mu_c)$. From Table 6, it may be seen that the observed and calculated rotational constants agree to within a few percent for both conformers at all levels of theory, confirming the overall geometry of the complex. However, neither form is clearly favored over the other.

Similarly, although not shown in the table, the calculated isotope shifts for both conformers at all levels of theory are within just a few megahertz of the experimental values. A table comparing the observed and calculated shifts is provided in the Supporting Information. Examination of that table reveals that, once again, although the changes in *A*, *B*, and *C* upon substitution confirm the basic geometry of Figure 3a, in most cases, they do not clearly distinguish between IA and IB. Only for CF₃SO₃H···D₂O do the isotope shifts show a distinct preference for IB. Correspondingly, the substitution coordinates derived from a Kraitchman analysis⁴⁵ also place the unbound water hydrogen atom in an orientation consistent with that of IB rather than of IA. Table 7 gives derived substitution coordinates, as determined by Kisiel's KRA program.⁴⁶

Note that it is not necessarily clear as to whether zero-point vibrational averaging even allows the two structures to be distinct. Indeed, as described above, after zero-point corrections, at the B2PLYP-D3BJ and DSD-PBEP86-D3BJ levels with the jun-cc-pVTZ basis, TS(I) is predicted to be more stable than either IA or IB by between 0.2 and 0.3 kcal/mol. Notwithstanding these ambiguities, however, we summarize by noting that the collective body of evidence (i.e., the overall agreement between the theory and experiment for the parent rotational constants (Table 6), as well as their shifts upon isotopic substitution and corresponding Kraitchman coordinates), support a structure in which the triflic acid hydrogen forms a primary hydrogen bond with the water oxygen, and a water hydrogen forms a secondary hydrogen

Table 7. Substitution Coordinates (in Å) for Triflic Acid Monohydrate Resulting from Kraitchman Analysis abc

	а	ь	с
S1	0.2314(65)	0.7942(19)	0.056(27)
IA	0.256129	0.782857	0.075261
IB	0.246873	0.799466	0.074599
Н3	1.72883(87)	-0.7045(21)	-0.8922(17)
IA	1.862187	-0.219931	-0.852885
IB	1.851872	-0.207230	-0.849588
H11	2.91614(52)	-2.03506(74)	$[0]^d$
IA	3.890051	-0.921159	-0.158536
IB	2.973671	-1.995789	-0.075238
H12	2.73965(55)	-0.6457(23)	0.8590(18)
IA	2.735745	-0.788804	0.856657
IB	2.717432	-0.795591	0.857094

"Atom numbering is shown in Figure 3a. ^bExperimentally derived substitution coordinates are in bold and uncertainties with Costain's error are quoted in parentheses. Signs were inferred based on the theoretical structures. Equilibrium coordinates are given for structures IA and IB from DSD-PBEP86-D3BJ/jun-cc-pVTZ optimized geometries. ^cWhen coordinates were obtained using either the parent or ³⁴S species, the fitted constants obtained from the individual fits of 0⁺ and 0⁻ tunneling states were averaged for the analysis. ^dThe resulting c-coordinate was an imaginary value and therefore set to zero.

bond to an oxygen of the triflic acid. The orientation of the unbound water hydrogen (in the parent species) is not well determined, though isotopic shifts in A, B, and C for $CF_3SO_3H\cdots D_2O$ and the substitution coordinates of the unbound water hydrogen atom favor an assignment of IB.

Triflic Acid Dihydrate. The four lowest energy conformers of the triflic acid dihydrate take on ringlike structures, which are shown in Figure 4. As with the monohydrate, the main difference between them involves the arrangement of the unbound hydrogen atoms. The two lowest energy forms, IIA and IIB, have alternating directions of the unbound OH bonds of water, while the two higher energy structures, IIC and IID, have the free water OH bonds oriented on the same side of the hydrogen-bonded ring. Among the levels of theory tested, these latter structures range from 0.20 to 0.87 kcal/mol higher in energy than the pair of structures that have alternating OH bond orientations. This preference for alternating free OH bond directions is similar to that previously encountered for HNO₃···(H₂O)₃.⁴⁷ The energy differences between the lowest energy structures, IIA and IIB, are very small, ranging from 0.03 to 0.18 kcal/mol across the levels of theory tested.

Similarly, energy differences between structures IIC and IID range from $\sim\!0.0$ to 0.15 kcal/mol. At all levels of theory employed, the most stable structure for the dihydrate is IIA. Attempts to identify a proton-transferred form did not converge to a stable minimum with all real frequencies, but rather reverted back to either IIA or IIB, depending on the theoretical method used.

Table 8 compares the calculated rotational constants with experimental results, again for two of the computational methods applied. (The full set of comparisons may be found in the Supporting Information.) Also given are the predicted dipole moment components along the a-, b-, and c-inertial axes of the parent isotopologue. As seen in the table, the calculated rotational constants are generally in agreement with experiment, again confirming the overall geometry of the complex. However, the similarity in the predicted rotational constants of the four conformers makes it difficult to arrive at a definitive assignment of the observed species based on rotational constants alone. 48 Comparisons between observed and calculated isotope shifts in rotational constants are provided in the Supporting Information and similarly concur with any of the structures given in Figure 4 but fail to decisively differentiate between them. All that said, there are a few noteworthy observations that favor an assignment to structure IIA. First, it can be seen that the predicted rotational constants for structures IIB and IID are almost always in rather poor agreement with the observed values compared with the corresponding values for IIA and IIC, suggesting that the observed species is not IIB or IID. Second, with IIA and IIC the most likely candidates, one of the key distinguishing factors is the expected rotational spectrum types. Observed a-type transitions were typically about 2-4 times more intense than *b*-type transitions, consistent with the ratio of $\mu_a/\mu_b > 1$ for IIA rather than the ratio of μ_a/μ_b < 1 for IIC. (See Table 8 for values of μ_a , μ_b , and μ_c .) Further, as noted above, despite thorough averaging and spectral searches, no c-type transitions were measured for the dihydrate, although they would have been expected to be easily observable for structure IIC based on the predicted dipole moment components. Note that the lack of symmetry makes it very unlikely that any largeamplitude motion would null out μ_c or significantly alter the values of μ_a and μ_b . Thus, combined with the result that IIA is consistently predicted as the global minimum structure and IIC one of the two highest energy structures, it would appear that IIA is likely the observed conformer.

Triflic Acid Trihydrate. As with the monohydrate and dihydrate, the most stable geometries of the trihydrate are those with cyclic water arrangements involving the triflic acid hydrogen. Prakash and co-workers¹⁵ also found structures involving open chains of water molecules, but they were of

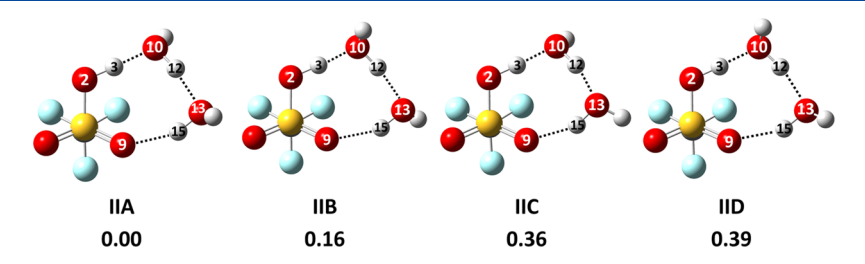


Figure 4. Four lowest energy conformers of $CF_3SO_3H\cdots(H_2O)_2$ calculated at the DSD-PBEP86-D3BJ/jun-cc-pVTZ level of theory. Numbers give relative energies in kcal/mol after zero-point corrections. Structure IIA is the lowest energy conformer of the four presented. IIB is higher in energy than IIA by 0.16 kcal/mol. A complete tabulation of conformer energies at all levels of theory used is given in Table 4.

 $\begin{tabular}{l} Table 8. Comparison of Observed Rotational Constants for Parent Triflic Acid Dihydrate and Theoretical Values for Predicted Conformers \end{tabular} absolute to the conformers \en$

			B2PLYP-D3BJ	DSD-PBEP86-D3BJ	RMS
			jun-cc-pVTZ ^d	jun-cc-pVTZ ^d	
A (observed)		1467.5486(28)			
IIA			1444	1451	2.
			1447	1455	2.
IIB			1400	1393	5.
			1398	1391	6.
IIC			1465	1477	1.
			1473	1485	1.
IID			1419	1406	4.
			1425	1412	4.
B (observed)		730.94197(26)			
IIA			735	741	2.
			729	735	1.
IIB			764	784	10.
			762	782	9.
IIC			730	735	1.
			723	729	1.
IID			742	765	7.
			730	753	5.
C (observed)		691.42664(21)			
IIA			693	698	1.
			688	692	1.
IIB			709	721	5.
			704	716	4.
IIC			684	686	0.
			677	679	1.
IID			700	713	4.
			691	704	3.
$ \mu_a $		$\neq 0^f$			
$ \mu_b $					
$ \mu_c $		$\ll \mu_a, \mu_b^f$			
IIA	(μ_a, μ_b, μ_c)		(3.5, 2.3, 0.1)	(3.4, 2.2, 0.1)	
IIB	(μ_a, μ_b, μ_c)		(3.6, 2.1, 0.8)	(3.6, 2.1, 0.8)	
IIC	(μ_a, μ_b, μ_c)		(2.7, 3.8, 1.5)	(2.7, 3.8,1.7)	
IID	(μ_a, μ_b, μ_c)		(4.7, 0.4, 0.5)	(4.8, 0.3, 0.3)	

"Fitted rotational constants and qualitative observations about the dipole moment components are in bold. Table 2 shows the complete set of fitted spectroscopic constants for triflic acid dihydrate. Rotational constants are in MHz. Dipole moment components are in debye. Equilibrium rotational constants calculated for each level of theory are presented in the first row for A, B, and C. Vibrational ground-state rotational constants were calculated using the vibrational corrections at the B3LYP-D3BJ/jun-cc-pVDZ level/basis and are given in the second row for A, B, and C. The lowest energy conformer is consistently calculated to be IIA. For calculations using the jun-cc-pVDZ or jun-cc-pVTZ basis sets, the jun-cc-pV(D+d)Z or jun-cc-pV(T+d)Z basis set was used on the sulfur atom, respectively. RMS percent deviation of calculated rotational constants relative to the observed values among the five levels of theory used. The Supporting Information shows a full table of calculated rotational constants. From the observation of a- and b-type transitions. No c-type transitions were observed.

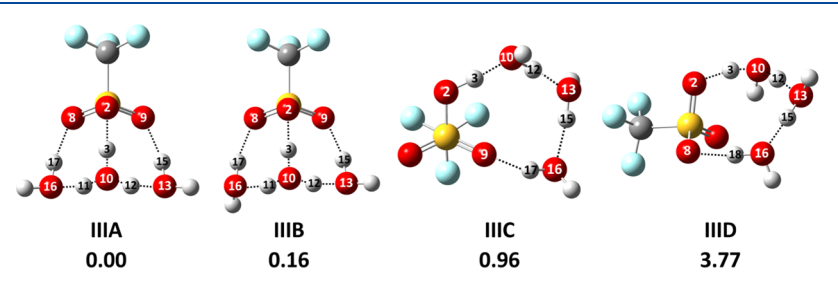


Figure 5. Four minimum energy structures of $CF_3SO_3H\cdots(H_2O)_3$ calculated at the DSD-PBEP86-D3BJ/jun-cc-pVTZ level of theory. Numbers give the relative energies in kcal/mol after zero-point corrections. Structure IIIA is the lowest energy conformer of the four structures shown (the next lowest energy conformer is structure IIIB, which is 0.16 kcal/mol higher in energy than structure IIIA with zero-point energy corrections). A complete tabulation of conformer energies at all levels of theory used is given in Table 4.

higher energy and are not considered here. While there are many possible conformers arising from the various possible orientations of the unbound hydrogen atoms, the four relevant and distinct lowest energy conformers are considered here and

Table 9. Comparison of Observed Rotational Constants for Parent Triflic Acid Trihydrate and Theoretical Values for Predicted Conformers abc

			B2PLYP-D3BJ	DSD-PBEP86-D3BJ	RMS%
			jun-cc-pVTZ ^d	jun-cc-pVTZ ^d	
A (observed)		1353.4599(50)			
IIIA			1366	1370	1.2
			1356	1360	0.5
IIIB			1366	1372	1.4
			1353	1359	0.6
IIIC			1019	1021	24.8
			1014	1017	25.1
IIID			1479	1483	8.4
			1415	1420	3.8
B (observed)		546.99304(30)			
IIIA			543	546	1.2
			541	544	1.5
IIIB			543	546	1.2
			541	544	1.4
IIIC			619	636	17.7
			625	642	18.8
IIID			512	518	5.5
			497	502	8.0
C (observed)		482.05570(23)			
IIIA			480	483	0.7
			477	480	1.0
IIIB			481	484	0.7
			478	481	0.9
IIIC			558	568	18.5
			560	570	18.9
IIID			444	448	7.0
			427	432	10.2
$ \mu_a $		$ \neq 0^f \ll \mu_{a}, \mu_c^f \neq 0^f $			
$ \mu_b $		$\ll \mu_a, \mu_c^f$			
$ \mu_c $		$\neq 0^f$			
IIIA	(μ_a, μ_b, μ_c)		(4.3, 0.0, 1.3)	(4.3, 0.0, 1.4)	
IIIB	(μ_a, μ_b, μ_c)		(4.8, 1.3, 0.4)	(4.8, 1.3, 0.4)	
IIIC	(μ_a, μ_b, μ_c)		(4.4, 0.5, 0.2)	(4.4, 0.5, 0.1)	
IIID	(μ_a, μ_b, μ_c)		(4.9, 1.0, 0.3)	(4.9, 1.0, 0.3)	

"Fitted rotational constants and qualitative observations about the dipole moment components are in bold. Table 3 shows the complete set of fitted spectroscopic constants for triflic acid trihydrate. Rotational constants are in MHz. Dipole moment components are in debye. Equilibrium rotational constants calculated for each level of theory are presented in the first row for A, B, and C. Vibrational ground-state rotational constants were calculated using the vibrational corrections at the B3LYP-D3BJ/jun-cc-pVDZ level/basis and are given in the second row for A, B, and C. The lowest energy conformer is consistently calculated to be IIIA. For calculations using jun-cc-pVDZ or jun-cc-pVTZ basis sets, jun-cc-pV(D+d)Z or jun-cc-pV(T+d)Z basis sets were used on the sulfur atom, respectively. RMS percent deviation of calculated rotational constants relative to the observed values among the five levels of theory used. The Supporting Information shows a full table of calculated rotational constants. From the observation of a- and c-type transitions. No b-type transitions were observed.

are shown in Figure 5. IIIA and IIIB are the lowest energy structures and are seen to feature a transfer of the triflic acid proton to a water molecule. IIIB corresponds to the structure labeled TAW_{3a} by Prakash et al., ¹⁵ with the H_3O^+ ion flanked by two water molecules in an $H_2O-H_3O^+-H_2O$ arrangement. IIIA differs only in the orientation of the unbound water hydrogens. IIID is also a proton-transferred structure and corresponds to Prakash's TAW_{3b} , with an $H_3O^+-H_2O-H_2O$ sequence of hydronium and water. IIIC is a hydrogen-bonded species, analogous to those seen in the dihydrate. IIIC and IIID lie higher in energy than IIIA and IIIB by 0.8-4.6~ kcal/mol. IIIA is predicted by the five sets of calculations shown in Table 4 to be the most stable conformer, with IIIB lying only about 0.10-0.17~ kcal/mol higher in energy.

Table 9 compares the observed rotational constants with those calculated at two levels of theory for the conformers shown in Figure 5. (Comparisons with the other levels of theory used appear in the Supporting Information.) From Table 9, it may be seen that the observed A rotational constants are in much better agreement with the lower-energy proton-transferred structures (IIIA and IIIB) than with the higher energy forms (IIIC and IIID), and that the B and C rotational constants also clearly exclude IIIC and IIID. Thus, while the rotational constants alone leave some ambiguity as to the orientation of the free hydrogens (i.e., IIIA vs IIIB), they allow the observed species to be clearly assigned to a hydrated ion pair. Further experimental evidence, however, allows for a clearer differentiation between these species. Specifically, given the calculated dipole moment components (μ_a , μ_b , and μ_c) Table 9), the absence of *b*-type transitions noted above and the observation of two c-type transitions argues for IIIA as the observed species. It is possible that vibrational averaging over

large-amplitude coordinates could affect dipole moment components, but in the absence of observable internal dynamics, it seems more likely that these arguments based on observed transition types should apply. In any case, since IIIA and IIIB are proton-transferred structures, the conclusion is essentially the same, namely that the observed form of the trihydrate is, indeed, a microsolvated ion pair. It is satisfying that, at all levels of theory employed, IIIA is the lowest energy structure, though again, the calculated energy differences between IIIA and IIIB are small.

DISCUSSION

Structural Signatures. It is apparent from Figures 3 and 4 that the mono- and dihydrates involve a hydrogen bond between the OH group of the triflic acid and a nearby water oxygen, while the lowest energy forms of the trihydrate (Figure 5) contain an H₃O⁺ moiety formed from the transfer of the triflic acid proton to water. As noted above, this is consistent with previously published theoretical results. The dihydrate exhibits the common motif (described as "homodromic rings" by Xantheas and co-workers that involves a cyclic hydrogen-bonded geometry. The distinction between hydrogen-bonded and proton-transferred structures is readily seen by examining the length of the triflic acid OH bond (O2–H3) and the distance between the triflic acid hydrogen and the nearest water oxygen (H3···O10) for the lowest energy structures. These are summarized in Table 10.

Table 10. Bond Distances and Proton Transfer Parameters for the Lowest Energy Structures of Triflic Acid Mono-, Di-, and Trihydrates ab

	monohydrate	dihydrate	trihydrate
triflic acid O-H distance (O2-H3)	1.007-1.016	1.040-1.057	1.517-1.547
hydrogen bond length (O3···H10)	1.580-1.621	1.417-1.478	1.024-1.031
$ ho_{ ext{PT}}$	-0.52 to -0.55	-0.31 to -0.38	+0.54 to +0.59
free triflic acid $(O-H)$	0.968-0.977		
free H_3O^+ (O-H)	1.019-1.043		

"All distances in Å. b Values in the table are based on calculated equilibrium structures and indicate the range across all five levels of theory used. OH distances and $\rho_{\rm PT}$ values for each level of theory are included in the Supporting Information.

Also included in the table are the calculated O–H bond lengths for free triflic acid and $\rm H_3O^+$. It is apparent that in the mono- and dihydrates, H3 is much closer to the triflic acid oxygen (O2), with a distance that is only slightly larger than that in free triflic acid. The hydrogen bond lengths (O3···H10) of 1.4–1.6 Å correspond to short hydrogen bonds. In contrast, the O3···H10 distance abruptly changes in the lowest energy form of the trihydrate to that in the $\rm H_3O^+$ cation, while the O2···H3 distance becomes very similar to that of short hydrogen bonds seen in the mono- and dihydrates.

The degree of proton transfer in these systems can be further quantified using the proton transfer parameter, $\rho_{\rm PT}$, defined by Kurnig and Scheiner, ⁵⁰ and originally applied to amine—hydrogen halide complexes, but later adapted to the study of acid—water systems ^{47,51}

$$\rho_{\rm PT} = (r_{\rm O2-H3}^{\rm complex} - r_{\rm O2-H3}^{\rm free}) - (r_{\rm H3-O10}^{\rm complex} - r_{\rm H3-O10}^{\rm free}) \tag{1}$$

Here, atom numbering follows that in Figures 3–5. r_{O2-H3}^{free} and $r_{O2-H3}^{complex}$ are OH bond distances in the free and complexed triflic acid, respectively, and r_{H3-O10}^{free} and $r_{H3-O10}^{complex}$ are the distances between the triflic acid hydrogen and the nearest water oxygen. (In the limit of complete proton transfer, $r_{O3-H10}^{complex}$ is equal to the OH bond length in free H₃O⁺.) When the degree of proton transfer is small, the first term is negligible and the second term is positive, so that $\rho_{\rm PT}$ is negative. In the event of substantial proton transfer, the second term is negligible and the first term is positive, so that $\rho_{\rm PT}$ is positive. The ranges of the computed values of $\rho_{\rm PT}$ for the lowest energy forms across the levels of theory employed are given for the mono-, di-, and trihydrates in Table 10. The ranges are seen to be small, and the negative values for the mono- and dihydrates indicate that they are best regarded as hydrogen-bonded species. In contrast, the range of positive values for the lowest energy structure of the trihydrate $(\rho_{PT} = 0.54 - 0.59 \text{ Å})$ is best regarded as having undergone proton transfer. Interestingly, ρ_{PT} for structure IIID is in the 0.30-0.45 Å range, confirming that it, too, involves proton transfer, albeit perhaps to a somewhat lesser extent than IIIA or IIIB. By way of comparison, the ρ_{PT} values for $HNO_3 \cdots (H_2O)_n$ (obtained at the MP2/6-311++G(2df,2pd) level) are -0.78, -0.64, and -0.54 Å for n = 1, 2, and 3, respectively. Individual values of ρ_{PT} obtained at each level of theory for every conformer are included in the Supporting Information.

Energetic Considerations. It is interesting to consider whether it is possible to understand, in simple chemical terms, the origin of differences in the minimum hydration numbers necessary to bring about ionization in acid-water clusters. For triflic acid, the minimum number appears to be three, whereas in the case of $(HNO_3)\cdots(H_2O)_n$ calculations indicate that n=4 is the smallest hydrate for which the solvated ion pair appears as a local (albeit not a global) minimum on the potential energy surface. For the latter system, simple energetic considerations have been able to rationalize this result.1 Here, we use similar arguments to understand the difference between the two acids. As in the case of HNO₃, we conceptualize the formation of the hydrated ion pair as involving removal of the proton from the acid, attachment of that proton to a water molecule, formation of a hydrated proton, $H_3O^+(H_2O)_{n-1}$, and the realization of the Coulomb stabilization when the $CF_3SO_3^-$ anion and the $H_3O^+(H_2O)_{n-1}$ cation are brought together in the complex. The number of hydrogen bonds in the final complex plays an additional role in understanding the energetics. There are two distinct issues: (i) the stability of the contact ion pair relative to that of the isolated monomers and (ii) the relative stabilities of the contact ion pair and the hydrogen-bonded complex.

Stability of the Contact Ion Pair Relative to the Free Monomers. From measured proton affinities, 52 we have

$$CF_3SO_3H \rightarrow H^+ + CF_3SO_3^-; \quad \Delta H_2 = 305 \text{ kcal/mol}$$
 (2)

$$H_2O + H^+ \to H_3O^+; \quad \Delta H_3 = -165 \text{ kcal/mol}$$
 (3)

Thus, the direct transfer of a proton from triflic acid to water is endothermic by 140 kcal/mol, i.e.

$$CE_3SO_3H + H_2O \rightarrow CE_3SO_3^- + H_3O^+; \quad \Delta H_4 = 140 \text{ kcal/mol}$$
 (4)

The equivalent calculation for HNO₃ yields a value of 160 kcal/mol.¹

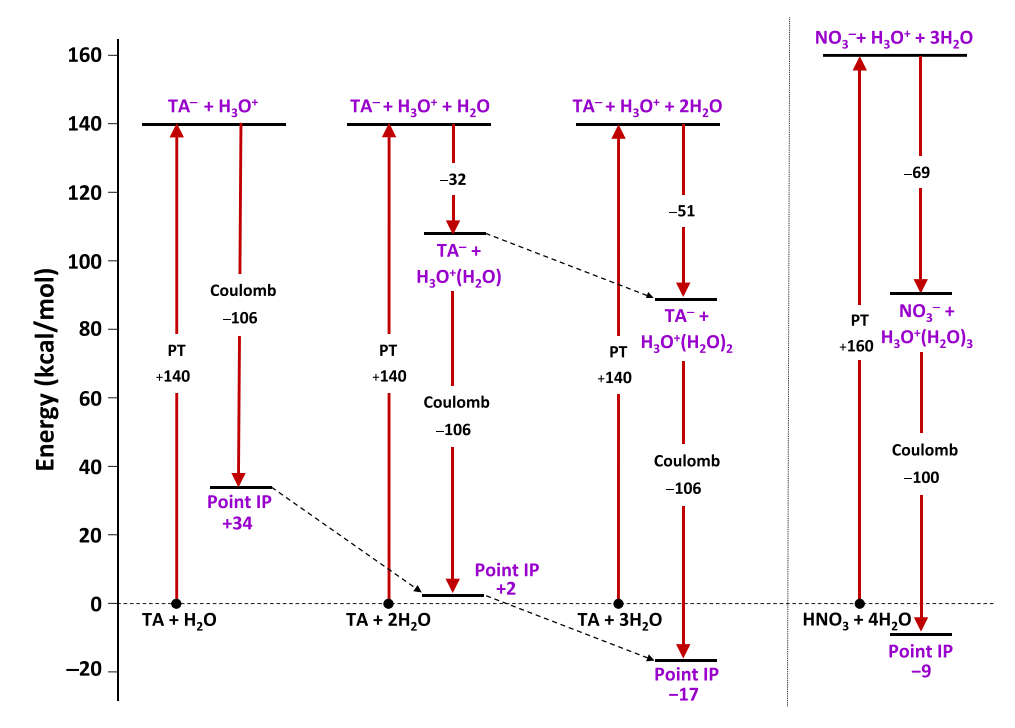


Figure 6. Approximate energy level diagram comparing the formation of point ion pairs for $CF_3SO_3H\cdots(H_2O)_{n=1-3}$. "TA" and "PT" refer to triflic acid and proton transfer, respectively. "Point IP" refers to an ion pair involving two-point charges, without additional hydrogen bond stabilization. For each value of n, the zero of energy is taken as that of the separated monomers. The dashed diagonal arrows track the stability of the separated and point ion pairs with successive hydration. The right side of the diagram shows the analogous energetics for the $NO_3^-\cdots H_3O^+(H_2O)_3$ system (see the text for discussion).

The energetics of the formation of several gas-phase proton hydrates have been experimentally quantified. 53-56 Using the results of Kebarle and co-workers, 53 we have

$$H_3O^+ + H_2O \rightarrow H_3O^+(H_2O); \quad \Delta H_5 = -31.6 \text{ kcal/mol}$$
 (5)

$$H_3O^+(H_2O) + H_2O \rightarrow H_3O^+(H_2O)_2; \quad \Delta H_6 = -19.5 \text{ kcal/mol}$$
 (6)

$$H_3O^+(H_2O)_2 + H_2O \rightarrow H_3O^+(H_2O)_3; \quad \Delta H_7 = -17.9 \text{ kcal/mol}$$
 (7)

From these data, we conclude that

$$H_3O^+ + 2H_2O \rightarrow H_3O^+(H_2O)_2; \quad \Delta H_8 = -51.1 \text{ kcal/mol}$$
 (8)

and

$$H_3O^+ + 3H_2O \rightarrow H_3O^+(H_2O)_3; \quad \Delta H_9 = -69.0 \text{ kcal/mol}$$
 (9)

Thus, once the triflic acid proton is transferred to a single H_2O molecule, the exothermicity associated with the hydration of H_3O^+ (eqs 5 and 8) partially offsets the endothermicity of the proton transfer to water (eq 4). The offset increases with the number of water molecules involved. The net process creates $CF_3SO_3^-$ and $H_3O^+(H_2O)_{n-1}$ at infinite separation.

These energetics are shown diagrammatically for $CF_3SO_3H + nH_2O$ (n = 1 - 3) in Figure 6. Also included (on the right side of the figure) is the corresponding diagram for $HNO_3 + 4H_2O$. It can be seen from the figure that for triflic acid with three water molecules, the energy of the separated ion pair $(CF_3SO_3^- + H_3O^+(H_2O)_2)$ is ~89 kcal/mol above that of the isolated monomers. In the case of HNO_3 , four water molecules are required to reach approximately the same energy. This arises because the larger proton transfer energy for HNO_3 (160 vs 140 kcal/mol) requires the additional stabilization provided by the formation of the $H_3O^+(H_2O)_3$ cation (eq 9). In short,

the 20 kcal/mol larger proton transfer energy for the $\rm HNO_3$ system is very nearly mitigated by the additional 17.9 kcal/mol stabilization associated with a fourth water molecule solvating the hydrated proton (eq 7).

Once the proton has been transferred, considerable further stabilization is realized by the Coulomb energy associated with bringing the separated ions to their distance in the complex, i.e., $q_1q_2/(4\pi\epsilon_0r)$. We refer to the resulting ion pair as the "point ion pair," whose energy includes the Coulomb energy associated with two point charges at a distance, r, but does not contain the hydrogen bond stabilization present in the final microsolvated system. While the above calculations are based on experimental data, the calculation of this energy involves considerable approximation insofar as the use of a single value of r is fictitious. In the case of the HNO₃···H₃O⁺(H₂O)₃, the value was taken as the distance between the nitrogen and the nearest oxygen of the H₃O⁺(H₂O)₃ (3.32 Å), giving a stabilization energy of ~100 kcal/mol, and thus bringing the energy to ~10 kcal/mol below that of the free monomers.

For triflic acid, the more extended mass distribution of the $CF_3SO_3^-$ anion relative to that of NO_3^- makes it less clear where to place the negative charge. However, if by analogy we choose r to be the calculated distance between the sulfur atom and the oxygen of the H_3O^+ moiety in $CF_3SO_3^-$... $H_3O^+(H_2O)_2$ (see Figure 5), we get a similar value of r=3.26 Å and hence a Coulomb stabilization energy of 102 kcal/mol (using the DSD-PBEP86-D3BJ/jun-cc-pVTZ coordinates). An alternative calculation involves retaining the positive charge on the H_3O^+ oxygen (whose formal charge is +1) and distributing the negative charge of the $CF_3SO_3^-$ anion over its three oxygen atoms, each of which has a formal charge of -1/3. The summed stabilization energy in this case is 106 kcal/mol, which is not too different but probably somewhat

better, as it arises from a slightly more nuanced model. Note that for the mono- and dihydrates, no ionized structures were identified computationally and thus there is no analogous value of r to use. However, if we assume a similar motif and similar atomic/ionic radii, we can again estimate a Coulomb stabilization of ~ 106 kcal/mol. With this value, it is seen from Figure 6 that, given the higher energy of the separated ion pairs for the mono- and dihydrates, the Coulomb energy does not render the ionized structure more stable than that of the isolated monomers. On this basis, it is not too surprising that they do not exist. However, as also seen in the figure, the -106 kcal/mol Coulomb energy is sufficient to bring the energy of the point ion pair to ~ 17 kcal/mol below that of the free monomers at n=3.

Relative Stability of the Contact Ion Pair and the Hydrogen-Bonded Complex. The above arguments address the plausibility of the appearance of an ion pair in the triflic acid trihydrate, but they do not address the relative stability of the ionized and hydrogen-bonded structures (e.g., IIIA and IIIB vs IIIC). According to Figure 5, the hydrogen-bonded form of the complex contains four hydrogen bonds, and the ionized forms contain three new hydrogen bonds. (The internal hydrogen bonds of the H₃O⁺(H₂O)₂ cation are accounted for in ΔH_8 .) Note that new hydrogen bonds are inequivalent, particularly in the ion, because one involves the central H₃O⁺ of the hydrated proton whereas the other two involve peripheral waters. Nevertheless, if we assume an average hydrogen bond stabilization energy, $\Delta E_{\rm HB}$ (which includes both the triflic acid-water hydrogen bond and the H₂O-H₂O hydrogen bonds), the effect of hydrogen bonding can be visualized using the diagram shown in Figure 7. The

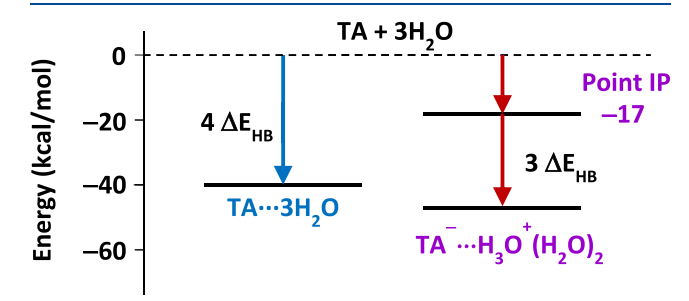


Figure 7. Energetics of the hydration of the point ion pair $CF_3SO_3^-\cdots H_3O^+(H_2O)_2$, assuming a hydrogen bond energy of ~ 10 kcal/mol (see the text for discussion).

zero of energy is taken as that of the isolated monomers $(CF_3SO_3H + 3H_2O)$, and the right side of the diagram shows that the point ion pair lies at the value estimated above, approximately -17 kcal/mol. From the figure, it can be seen that the ion paired form will be more stable than the hydrogenbonded form if $3\Delta E_{HB} + 17 > 4\Delta E_{HB}$, where ΔE_{HB} is the average hydrogen bond energy in the complex. In other words, if $\Delta E_{\rm HB}$ < 17 kcal/mol, the ionic form should be expected to be more stable. A hydrogen bond stabilization energy of 17 kcal/ mol is rather large for a typical hydrogen bond, and thus, it is likely that $\Delta E_{\rm HB}$ would, indeed, be less than 17 kcal/mol. For instance, in HNO₃-water clusters, an estimate of only 10 kcal/ mol per hydrogen bond was obtained,1 and for H3N-HF, the calculated binding energy is about -12 kcal/mol.⁵⁷ Alternatively, the average binding energy for the hydrogen-bonded form of the trihydrate (IIIC) may be estimated from the calculated binding energy divided by the number of hydrogen

bonds. With a range of binding energies from 25 to 46 kcal/mol (Table 4) and four hydrogen bonds (Figure 5), this gives the average hydrogen bond energy in the 6-12 kcal/mol range, still less than the critical value of 17 kcal/mol. In this light, it is entirely plausible that the energy of the proton-transferred complex would fall below that of the hydrogen-bonded system. We note that the energy difference between the hydrogen-bonded and ionized forms is small and is almost certainly within the expected accuracy of this model, given the underlying assumptions. Thus, despite the successful prediction in this case, what is probably more accurate to say is that at n=3, the energies of the neutral and ionized forms become comparable. That the ionized form wins as the lowest energy species lies in details that cannot necessarily be reliably captured at this level of analysis.

In summary, while the above arguments do not substitute for high-level computations, it is possible to qualitatively and semiquantitatively rationalize why three water molecules are required to render the microsolvated ion pair the lowest energy form of triflic acid trihydrate. It is interesting to note that the energetics for triflic acid are very similar to those of HNO3 except that the proton transfer energy is only 140 kcal/mol, whereas for HNO3, it is 160 kcal/mol. This requires less stabilization energy to offset the proton transfer energy and accounts for the need for only three water molecules to create a hydrated ion pair, i.e., $H_3O^+(H_2O)_2$... $SO_3CF_3^-$. It is, perhaps, surprising that such simple calculations work for these two acids, and it will be interesting to see if results for other acids can be similarly understood. Certainly, other factors such as conformational flexibility have been identified in the case of sulfur oxoacids9 and, more generally, the roles of entropy and finite cluster temperature need to be considered for a complete description. Nevertheless, similar arguments have recently been applied to quantitatively rationalize why the triflic acidtrimethylamine system exists as a trimethylammonium triflate ion pair (CF₃SO₃⁻···⁺HN(CH₃)₃) in the gas phase.⁵⁸

CONCLUSIONS

Supersonic jet microwave spectra have been obtained for the complexes of triflic acid (CF₃SO₃H) with one, two, and three water molecules, and the results have been compared with a series of DFT calculations. For each hydrate, several lowenergy conformers are predicted. For the monohydrate, the microwave spectra are consistent with one of the two nearly isoenergetic structures. For both the di- and trihydrates, the spectra are consistent with the lowest energy form. Both the monohydrate and dihydrate are hydrogen-bonded systems, with no evidence of proton transfer from the triflic acid to water in any of the calculated conformers. However, for the trihydrate, the lowest energy conformers consist of a hydrated hydronium triflate ion pair. Thus, three water molecules are needed for triflic acid to ionize in a cold microsolvated cluster. This number is on the low end of the range that is typical for other simple protic acids and likely results from the unusually strong acidity of triflic acid.

A simple thermodynamic calculation based on proton affinities, Coulomb energy, and hydrogen bond strength can be used to rationalize this result. This involves consideration of the proton transfer energy, the formation energy for an Eigenlike cation, and the Coulomb energy when the separated ions are brought to their distance in the complex. Hydrogen bond stabilization plays an additional role, but the primary effect is that the energy of formation of the hydrated proton increases

with increasing n and allows the Coulomb stabilization to bring the energy of the point ion pair to a value lower than that of the sum of the free monomer energies. This is the second case in which such a calculation has successfully rationalized the number of water molecules needed before a simple protic acid ionizes in a small aqueous cluster (the first being HNO₃). It will be interesting in subsequent work to test its applicability to other strong acids that ionize in bulk solution.

ASSOCIATED CONTENT

Solution Supporting Information

The Supporting Information is available free of charge at https://pubs.acs.org/doi/10.1021/acs.jpca.1c06815.

Tables of observed spectral frequencies and residuals from the least-squares fits; Cartesian coordinates; computed rotational constants, isotope shifts of the rotational constants, selected bond lengths, and $\rho_{\rm PT}$ values at all levels of theory employed (PDF)

AUTHOR INFORMATION

Corresponding Author

Kenneth R. Leopold — Department of Chemistry, University of Minnesota, Minneapolis, Minnesota 55455, United States; orcid.org/0000-0003-0800-5458; Email: kleopold@umn.edu

Authors

 Anna K. Huff – Department of Chemistry, University of Minnesota, Minneapolis, Minnesota 55455, United States
 Nathan Love – Department of Chemistry, University of Minnesota, Minneapolis, Minnesota 55455, United States

Complete contact information is available at: https://pubs.acs.org/10.1021/acs.jpca.1c06815

Notes

The authors declare no competing financial interest.

ACKNOWLEDGMENTS

This work was supported by the National Science Foundation (Grant nos. CHE 1563324 and CHE 1953528) and the Minnesota Supercomputing Institute. N.L. was supported, in part, by a Lester C. and Joan Krogh-Excellence Fellowship at the University of Minnesota.

■ REFERENCES

- (1) Leopold, K. R. Hydrated Acid Complexes. Annu. Rev. Phys. Chem. 2011, 62, 327-349. and references therein
- (2) Forbert, H.; Masia, M.; Kaczmarek-Kedziera, A.; Nair, N. N.; Marx, D. Aggregation-Induced Chemical Reactions: Acid Dissociation in Growing Water Clusters. J. Am. Chem. Soc. 2011, 133, 4062–4072.
- (3) Lin, W.; Paesani, F. Infrared Spectra of HCl(H₂O)n Clusters from Semiempirical Born-Oppenheimer Molecular Dynamics Simulations. J. Phys. Chem. A 2015, 119, 4450–4456.
- (4) Vargas-Caamal, A.; Cabellos, J. L.; Ortiz-Chi, F.; Rzepa, H. S.; Restrepo, A.; Merino, G. How Many Water Molecules Does it Take to Dissociate HCl? *Chem. Eur. J.* **2016**, 2812.
- (5) Elena, A. M.; Meloni, S.; Ciccotti, G. Equilibrium and Rate Constants, and Reaction Mechanism of the HF Dissociation in the $HF(H_2O)_7$ Cluster by ab Initio Rare Event Simulations. *J. Phys. Chem.* A **2013**, *117*, 13039–13050.
- (6) Lengyel, J.; Ončák, M.; Fedor, J.; Kočišek, J.; Pysanenko, A.; Beyer, M. K.; Fárnik, M. Electron-Triggered Chemistry in HNO₃/H₂O Complexes. *Phys. Chem. Chem. Phys.* **2017**, *19*, 11753–11758.

- (7) Temelso, B.; Morrell, T. E.; Shields, R. M.; Allodi, M. A.; Wood, E. K.; Kirschner, K. N.; Castonguay, T. C.; Archer, K. A.; Shields, G. C. Quantum Mechanical Study of Sulfuric Acid Hydration: Atmospheric Implications. *J. Phys. Chem. A* **2012**, *116*, 2209–2224.
- (8) Temelso, B.; Phan, T. N.; Shields, G. C. Computational Study of the Hydration of Sulfuric Acid Dimers: Implications for Acid Dissociation and Aerosol Formation. *J. Phys. Chem. A* **2012**, *116*, 9745–9758
- (9) Chung, Y. K.; Kim, K. S. Dissociation of Sulfur Oxoacids by Two Water Molecules Studied Using ab Initio and Density Functional Theory Calculations. *Int. J. Quantum Chem.* **2017**, No. e25419.
- (10) Krishnakumar, P.; Maity, D. K. Microhydration of a Benzoic Acid Molecule and its Dissociation. *New. J. Chem.* **2017**, *41*, 7195–7202.
- (11) Krishnakumar, P.; Maity, D. K. Theoretical Studies on Dimerization vs. Microhydration of Carboxylic Acids. *Comput. Theor. Chem.* **2017**, *1099*, 185–194.
- (12) Krishnakumar, P.; Maity, D. K. Microhydration of Oxalic Acid Leading to Dissociation. *Mol. Phys.* **2017**, *115*, 3224–3233.
- (13) Krishnakumar, P.; Maity, D. K. Effect of Microhydration on Dissociation of Trifluoroacetic Acid. *J. Phys. Chem. A* **2014**, *118*, 5443–5453.
- (14) Wang, C.; Clark, J. K., II; Kumar, M.; Paddison, S. J. An *Ab Initio* Study of the Primary Hydration and Proton Transfer of CF₃SO₃H and CF₃O(CF₂)₂SO₃H: Effects of the Hybrid Functional and Inclusion of Diffuse Functions. *Solid State Ionics* **2011**, *199*–200, 6–13.
- (15) Prakash, M.; Subramanian, V. *Ab Initio* and Density Functional Theory (DFT) Studies on Triflic Acid with Water and Protonated Water Clusters. *I. Mol. Model.* **2016**, 22, No. 293.
- (16) Sepehr, F.; Paddison, S. J. Primary Hydration and Proton Transfer of Electrolyte Acids: An Ab Initio Study. *Solid State Ionics* **2017**, *306*, 2–12.
- (17) Olah, G.; Prakash, F.; Sommer, J. Superacids. Science 1979, 206, 13-20.
- (18) Saito, S.; Saito, S.; Ohwada, T.; Shudo, K. The Hammett Acidity Function H_o of Trifluoromethanesulfonic Acid-Trifluoroacetic Acid and Related Acid Systems. A Versatile Nonaqueous Acid System. *Chem. Pharm. Bull.* **1991**, 39, 2718–2720.
- (19) Kazakova, A. N.; Vasilyev, A. V. Trifluoromethanesulfonic Acid in Organic Synthesis. *Russ. J. Org. Chem.* **2017**, *53*, 485–509.
- (20) Li, S.; Tao, F.-M.; Gu, R. Theoretical Study on the Ionic Dissociation of Halosulfonic Acids in Small Water Clusters. *Chem. Phys. Lett.* **2006**, 426, 1–7.
- (21) Spencer, J. B.; Lundgren, J.-O. Hydrogen Bond Studies LXXIII. The Crystal Structure of Trifluoromethanesulphonic Acid Monohydrate, H₃O⁺CF₃SO₃⁻ at 298 and 83°K. *Acta Crystallogr., Sect. B: Struct. Crystallogr. Cryst. Chem.* **1973**, 29, 1923–1928.
- (22) Delaplane, R. G.; Lundgren, J.-O.; Olovsson, I. Hydrogen Bond Studies. XCVII. The Crystal Structure of Trifluoromethanesulphonic Acid Dihydrate, H₅O₂⁺CF₃SO₃⁻, at 225 and 85 K. *Acta Crystallogr. Sect. B: Struct. Crystallogr. Cryst. Chem.* **1975**, 31, 2202–2207.
- (23) Lundgren, J.-O. Hydrogen Bond Studies. CXXX. The Crystal Structure of Trifluoromethanesulphonic Acid Tetrahydrate, $H_9O_4^+CF_3SO_3^-$. Acta Crystallogr., Sect. B: Struct. Crystallogr. Cryst. Chem. 1978, 34, 2428–2431.
- (24) Delaplane, R. G.; Lundgren, J.-O.; Olovsson, I. Hydrogen Bond Studies. CVI. The Crystal Structure of 2CF₃SO₃H·H₂O. *Acta Crystallogr., Sect. B: Struct. Crystallogr. Cryst. Chem.* **1975**, 31, 2208–2213.
- (25) Vener, M. V.; Chernyshov, I. Y.; Rykounov, A. A.; Filarowski, A. Structural and Spectroscopic Features of Proton Hydrates in the Crystalline State. Solid-State DFT Study on HCl and Triflic Acid Hydrates. *Mol. Phys.* **2018**, *116*, 251–262.
- (26) Hayes, R. L.; Paddison, S. J.; Tuckerman, M. E. Proton Transport in Triflic Acid Pentahydrate Studied via Ab Initio Path Integral Molecular Dynamics. *J. Phys. Chem. A* **2011**, *115*, 6112–6124.

- (27) Hayes, R. L.; Paddison, S. J.; Tuckerman, M. E. Proton Transfer in Triflic Acid Hydrates Studied via Path Integral Car-Parrinello Molecular Dynamics. *J. Phys. Chem. B* **2009**, *113*, 16574–16589.
- (28) Kreuer, K.-D.; Paddison, S. J.; Spohr, E.; Schuster, M. Transport in Proton Conductors for Fuel-Cell Applications: Simulations, Elementary Reactions, and Phenomenology. *Chem. Rev.* **2004**, *104*, 4637–4678.
- (29) Balle, T. J.; Flygare, W. H. Fabry-Perot Cavity Pulsed Fourier Transform Microwave Spectrometer with a Pulsed Nozzle Particle Source. *Rev. Sci. Instrum.* **1981**, *52*, 33–45.
- (30) Brown, G. G.; Dian, B. C.; Douglass, K. O.; Geyer, S. M.; Shipman, S. T.; Pate, B. H. A Broadband Fourier Transform Microwave Spectrometer Based on Chirped Pulse Excitation. *Rev. Sci. Instrum.* **2008**, *79*, No. 053103.
- (31) Phillips, J. A.; Canagaratna, M.; Goodfriend, H.; Grushow, A.; Almlöf, J.; Leopold, K. R. Microwave and Ab Initio Investigation of HF-BF₃. J. Am. Chem. Soc. **1995**, 117, 12549–12556.
- (32) Dewberry, C. T.; Mackenzie, R. B.; Green, S.; Leopold, K. R. 3D-Printed Slit Nozzles for Fourier Transform Microwave Spectroscopy. *Rev. Sci. Instrum.* **2015**, *86*, No. 065107.
- (33) Canagaratna, M.; Phillips, J. A.; Goodfriend, H.; Leopold, K. R. Structure and Bonding of the Sulfamic Acid Zwitterion: Microwave Spectrum of ⁺H₃N-SO₃⁻. *J. Am. Chem. Soc.* **1996**, *118*, 5290–5295.
- (34) Canagaratna, M.; Phillips, J. A.; Ott, M. E.; Leopold, K. R. The Nitric Acid-Water Complex: Microwave Spectrum, Structure, and Tunneling. J. Phys. Chem. A 1998, 102, 1489–1497.
- (35) Watson, J. K. G. Aspects of Quartic and Sextic Centrifugal Effects on Rotational Energy Levels. In *Vibrational Spectra and Structure*; Durig, J. R., Ed.; Elsevier Scientific Publishing: Amsterdam, 1977; pp 1–89.
- (36) Pickett, H. M. The Fitting and Prediction of Vibration-Rotation Spectra with Spin Interactions. *J. Mol. Spectrosc.* **1991**, *148*, 371–377.
- (37) Frisch, M. J.; Trucks, G. W.; Schlegel, H. B.; Scuseria, G. E.; Robb, M. A.; Cheeseman, J. R.; Scalmani, G.; Barone, V.; Petersson, G. A.; Nakatsuji, X. L. et al. *Gaussian 16*; Gaussian, Inc.: Wallingford, CT, 2016.
- (38) Xie, F.; Fuse, M.; Hazrah, A. S.; Jäger, W.; Barone, V.; Xu, Y. Discovering the Elusive Global Minimum in a Ternary Chiral Cluster: Rotational Spectra of Propylene Oxide Trimer. *Angew. Chem., Int. Ed.* **2020**, *59*, 22427–22430.
- (39) Grimme, S.; Ehrlich, S.; Goerigk, L. Effect of the Damping Function in Dispersion Corrected Density Functional Theory. *J. Comput. Chem.* **2011**, 32, 1456–1465.
- (40) Becke, A. D.; Johnson, E. R. A Density-Functional Model of the Dipsersion Interaction. *J. Chem. Phys.* **2005**, *123*, No. 154101.
- (41) Puzzarini, C.; Bloino, J.; Tasinato, N.; Barone, V. Accuracy and Interpretability: The Devil and the Holy Grail. New Routes across Old Boundaries in Computational Spectroscopy. *Chem. Rev.* **2019**, *119*, 8131–8191.
- (42) Penocchio, E.; Piccardo, M.; Barone, V. Semiexperimental Equilibrium Structures for Building Blocks of Organic and Biological Molecules: The B2PLYP Route. *J. Chem. Theory Comput.* **2015**, *11*, 4689–4707.
- (43) Santra, G.; Sylvetsky, N.; Martin, J. M. L. Minimally Empirical Double-Hybrid Functionals Trained against the GMTKN55 Database: revDSD-PBEP86-D4, revDOD-PBE-D4, and DOD-SCAN-D4. *J. Phys. Chem. A* **2019**, *123*, 5129–5143.
- (44) Pritchard, B. P.; Altarawy, D.; Didier, B.; Gibson, T. D.; Windus, T. L. A New Basis Set Exchange: An Open, Up-to-date Resource for the Molecular Sciences Community. *J. Chem. Inf. Model.* **2019**, *59*, 4814–4820.
- (45) Kraitchman, J. Determination of Molecular Structure from Microwave Spectroscopic Data. Am. J. Phys. 1953, 21, 17–24.
- (46) The KRA program, written by Z. Kisiel, may be downloaded from http://www.ifpan.edu.pl/~kisiel/struct/struct.htm#kra.
- (47) Sedo, G.; Doran, J. L.; Leopold, K. R. Partial Proton Transfer in the Nitric Acid Trihydrate Complex. *J. Phys. Chem. A* **2009**, *113*, 11301–11310.

- (48) For the dihydrate, the only possible set of substitution coordinates (given the data) is for the sulfur atom, and this contains essentially no useful information. The biggest difference between IIA and IIC is in the c-coordinate, for which the equilibrium values are predicted to be 0.04 and 0.15 Å, respectively. Noting that these values are rather small, and that Kraitchman's equations are typically unreliable for substitution near an axis (indeed, the resulting substitution c-coordinate is imaginary), the similarity between these numbers precludes any meaningful interpretation.
- (49) McCurdy, P. R.; Hess, W. P.; Xantheas, S. S. Nitric Acid-Water Complexes: Theoretical Calculations and Comparison to Experiment. *J. Phys. Chem. A* **2002**, *106*, 7628–7635.
- (50) Kurnig, I. J.; Scheiner, S. Ab Initio Investigation of the Structure of Hydrogen Halide-Amine Complexes in the Gas Phase and in a Polarizable Medium. *Int. J. Quantum Chem.* **1987**, 32, 47–56.
- (51) Craddock, M. B.; Brauer, C. S.; Leopold, K. R. Microwave Spectrum, Structure, and Internal Dynamics of the Nitric Acid Dihydrate Complex. *J. Phys. Chem. A* **2008**, *112*, 488–496.
- (52) Lias, S. G.; Bartmess, J. E.; Liebman, J. F.; Holmes, J. L.; Levin, R. D.; Mallard, W. G. Ion Energetics Data. *NIST Chemistry WebBook*; National Institute of Standards and Technology: Gaithersburg, MD, 2021. http://webbook.nist.gov (retrieved July 4, 2021).
- (53) Lau, Y. K.; Ikuta, S.; Kebarle, P. Thermodynamics and Kinetics of the Gas-Phase Reactions: $H_3O^+(H_2O)_{n+1} + H_2O = H_3O^+(H_2O)_n$. *J. Am. Chem. Soc.* **1982**, *104*, 1462–1469.
- (54) Kebarle, P.; Searles, S. K.; Zolla, A.; Scarborough, J.; Arshadi, M. The Solvation of the Hydrogen Ion by Water Molecules in the Gas Phase. Heats and Energetics of Solvation of Individual Reactions $H^+(H_2O)_{n-1} + H_2O \rightarrow H^+(H_2O)_n$. *J. Am. Chem. Soc.* **1967**, 89, 6393–6399.
- (55) Cunningham, A. J.; Payzant, J. D.; Kebarle, P. A Kinetic Study of the Proton Hydrate $H^+(H_2O)_n$ Equilibria in the Gas Phase. *J. Am. Chem. Soc.* **1972**, *94*, 7627–7632.
- (56) Meot-Ner, M.; Field, F. H. Stability, Association, and Dissociation in the Cluster Ions $H_3S^+\cdot nH_2S$, $H_3O^+\cdot nH_2O$, and $H_2S^+\cdot H_2O$. *J. Am. Chem. Soc.* **1977**, *99*, 998–1003.
- (57) Hunt, S. W.; Higgins, K. J.; Craddock, M. B.; Brauer, C. S.; Leopold, K. R. Influence of a Polar Near Neighbor on Incipient Proton Transfer in a Strongly Hydrogen Bonded Complex. *J. Am. Chem. Soc.* **2003**, *125*, 13850–13860.
- (58) Love, N.; Huff, A. K.; Leopold, K. R. Proton Transfer in a Bare Superacid-Amine Complex: A Microwave and Computational Study of Trimethylammonium Triflate. *J. Phys. Chem. A* **2021**, *125*, 5061–5068